

# Simultaneous Calibration of Multiple Microphones for Both Phase and Amplitude in an Impedance Tube

Péter TÓTH<sup>(1),(2)</sup>, Christophe SCHRAM<sup>(2)</sup>

<sup>(1)</sup> *Department of Fluid Mechanics, Budapest University of Technology and Economics*  
H-1111 Budapest, Bertalan Lajos u. 4-6 Hungary; e-mail: tothp@vki.ac.be; toth@ara.bme.hu

<sup>(2)</sup> *von Karman Institute for Fluid Dynamics*  
Chaussée de Waterloo, 72 B-1640 Rhode-St-Genèse Belgium

(received October 31, 2013; accepted June 23, 2014)

This paper presents and compares microphone calibration methods for the simultaneous calibration of small electret microphones in a wave guide. The microphones are simultaneously calibrated to a reference microphone both in amplitude and phase. The calibration procedure is formulated on the basis of the damped plane wave propagation equation, from which the acoustics field along the wave guide is predicted, using several reference measurements. Different calibration models are presented and the methods were found to be sensitive to the formulation, as well as to the number of free parameters used during the reconstruction of the wave-field. The wave guide model based on five free parameters was found to be the preferred method for this type of calibration procedure.

**Keywords:** electret microphone, simultaneous microphone calibration, impedance-tube.

## 1. Introduction

Acoustic measurements often require the use of many microphones simultaneously. For example, arrays of microphones are used for source localisation, duct mode estimation, or source directivity measurements. The instrumentation needed for multiple microphone data logging has recently become broadly available, due to the decrease of the equipment cost of one microphone acquisition channel. The cost has been mostly reduced by the use of cheaper and easier to operate microphones, such as electret or mems microphones (HUMPHREYS *et al.*, 2003). Additionally, low cost digital microphone systems have recently become available (KULKA, 2011). The frequency response of these microphone capsules is not individually specified, meanwhile it can vary due to manufacturing tolerances or due to environmental conditions such as temperature. The array processing methods, such as source localisation with beamforming are sensitive to the phase and amplitude matching of acquisition channels (TASHEV, 2005). It was shown by YARDIBI *et al.* (2010) that the sensitivity error of the microphones translates one-to-one into the amplitude error of the beamforming source level prediction. In connection

with the signal phase error, YARDIBI *et al.* (2010) also showed that microphone position uncertainty, which causes a phase shift in the signal, decreases the prediction amplitude, in addition to a small localization error. Location error with a Gaussian distribution having a standard deviation of 14.6% of the wavelength (corresponding to a phase error of  $52.56^\circ$ ), caused beamforming amplitude decrease by approximately 3.5 dB compared to the true source level. Advanced beamforming algorithms are even more sensitive to microphone mismatch (TASHEV, 2005). Therefore, for reliable measurements, microphone or array calibration is necessary.

For beamforming microphone arrays, the microphone mismatches can be corrected by the array calibration procedure presented in (MUELLER, 2002). This requires an anechoic environment, and source and microphone positions need to be known. In case of the array is used in a non-ideal acoustic environment, such as an aerodynamic wind tunnel, or in field measurements, an acoustically treated enclosure should be used during the calibration. If the array is not a pre-assembled device, having known microphone positions, but the microphone positions can be varied, this type of calibration is inconvenient, especially when the microphone

positions are to be measured in an acoustical way, such as in the work of RAYKAR and DURAI SWAMI (2004). In this case pre-calibrated microphones would be easier to use and would also give a reliable starting point for method development. Other measurements, such as in-duct acoustic measurements also need phase and amplitude calibrated microphones, such as in the work of LOWIS *et al.* (2010).

Several microphone calibration methods are summarized in the work of ZUCKERWAR *et al.* (2006), but all of them are suitable for the calibration of one microphone channel at a time. Calibration of many microphones is time-consuming using these methods.

If the procedure of simultaneous calibration of microphones is easily available with sufficient accuracy then the calibration of the microphone channels can be repeated periodically, yielding to the tracking of the instrument, which is increasing measurement reliability.

The simultaneous calibration of several sensors using a multi-port tube calibrator is presented in (OLDHAM *et al.*, 2009). This calibration device produces the same acoustics field at the end of several small diameter tubes. One tube is reserved for a reference microphone and the transfer function (TF) of the unknown microphones are directly obtained from their comparison with the reference microphone signal. The idea can also be used for phase calibration, however the methodology was evaluated only for amplitude calibration with an accuracy of  $\pm 1$  dB up to 4.9 kHz and  $\pm 0.5$  dB up to 2 kHz within the confidence level of 95%. The method can be effectively used for in situ calibrations of the microphones, but only a few calibration tubes can be attached.

In the special case of in-duct acoustic measurements, when the microphones are uniformly spaced along the duct, the phase calibration of the microphones can be done in situ, assuming that the duct modes are mutually incoherent. In this case the phase difference between the microphones only depends on the distance between them, and the cross spectral matrix has to have a Töplitz structure (LOWIS *et al.*, 2010). The phase correction factors for the microphones can be determined in order to satisfy this property of the cross spectral matrix. A reasonable accuracy for the phase lags is achieved by the authors in (LOWIS *et al.*, 2010), however the sensitivity of the microphones is not determined in this way. A similar methodology is used for the phase and gain calibration of linear microphone arrays in the works of (PAULRAJ, KAILATH, 1985) and (SNG, LI, 2000).

In this paper we present methods to perform both the phase and the gain calibration of multiple microphones simultaneously using an impedance tube. The calibrations are based on the estimation and elimination of unknown model parameters of a waveguide model, providing a known wave field which is used for

the calculation of microphone correction factors along the waveguide.

The idea of estimating the acoustic model parameters in a waveguide with the help of several measurements is also applied in (BOONEN *et al.*, 2009; DE ROECK *et al.*, 2012).

The number of the model parameters depends on the measurement set-up. Several scenarios can be considered for microphone calibration. Three of them will be presented in the following, comparing of their accuracies and calculation complexities.

## 2. Theory

### 2.1. Acoustic wave propagation in a rigid wall wave-guide

For a circular waveguide, only plane waves propagate for frequencies lower than the first cut-on frequency of higher modes,  $f_c = 1.84c/2\pi r$ , where  $c$  is the speed of sound and  $r$  is the radius of the circular duct. These plane waves can be described by a 1D damped wave equation for the pressure fluctuation  $p'$ :

$$\frac{\partial^2 p'}{\partial t^2} = c^2 \frac{\partial^2 p'}{\partial x^2} - R \frac{\partial p'}{\partial t}. \quad (1)$$

The damping strength is represented by  $R$ . Similar equation can be written for the velocity fluctuations  $v'$ . In the frequency domain, the solution of the 1D homogeneous plane wave propagation has the following form for the pressure and the velocity fluctuation (WYLIE, STREETER, 1978):

$$p'(x, t) = e^{i\omega t} (Ae^{\gamma x} + Be^{-\gamma x}), \quad (2)$$

$$v'(x, t) = \frac{\omega}{i\rho c^2 \gamma} e^{i\omega t} (Ae^{\gamma x} - Be^{-\gamma x}), \quad (3)$$

where  $\omega$  is the angular frequency,  $A$  and  $B$  to be determined from the boundary conditions,  $\rho$  is the fluid density,  $i = \sqrt{-1}$  and  $\gamma = k(i + \zeta)$  is the propagation constant, including the wave number  $k = \omega/c$  and the attenuation constant  $\zeta$ . This frequency-independent model of the attenuation is a reasonable simplification of the propagation constant (BLAUERT, XIANG, 2008).

### 2.2. The calibration tube

The previously introduced general description of the waves is used to describe the fluid motion in the calibration tube, as presented in Fig. 1.

The calibration device is a rigid walled aluminium tube having a circular cross section of diameter 42 mm and wall thickness of 3 mm. The first microphone is placed at  $x_1 = 180$  mm, measured from the end of the waveguide where the acoustic impedance,  $Z_e$ , is mounted. On the opposite end of the tube a loudspeaker (Sp) is mounted. Along the length of the tube

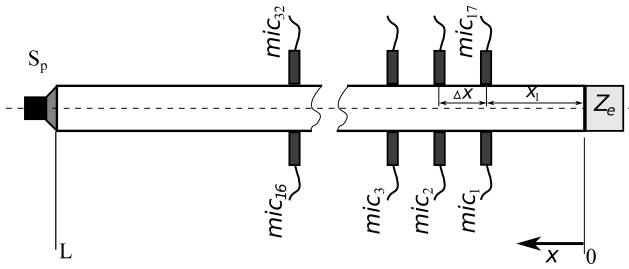


Fig. 1. Sketch of the calibration arrangement.

32 microphones can be placed in two rows. The microphones are placed with constant spacing  $\Delta x = 30$  mm. The diameter of the holes for the microphones is 3.0 mm. The microphones, located along the tube, are denoted by  $mic_l$  ( $l = 1..32$ ). The pipe length is approximately  $L = 3.6$  m.

### 2.3. Boundary conditions

Based on this calibration arrangement, boundary conditions for the wave propagation equations can be specified for obtaining  $A$  and  $B$ . At the tube termination,  $x = 0$ , the acoustic impedance is specified:

$$\frac{p'(0, t)}{v'(0, t)} = \frac{(A + B)Z_a(-1 + i\zeta)}{A - B} = Z_e, \quad (4)$$

where  $Z_a = \rho c$  is the characteristic impedance of the fluid in the tube. On the other end,  $x = L$ , a periodic excitation of the pressure is assumed to have the following form:

$$p'(L, t) = e^{i\omega t} (Ae^{\gamma L} + Be^{-\gamma L}) = A_0 e^{i\omega t}. \quad (5)$$

The amplitude of the excitation is  $A_0$ . Equations (4), (5) can be solved to give  $A$  and  $B$ :

$$A = \frac{-A_0(Z_e\omega + iZ_a c\gamma)}{e^{-\gamma L}(-Z_e\omega + iZ_a c\gamma) - e^{\gamma L}(Z_e\omega + iZ_a c\gamma)}, \quad (6)$$

$$B = \frac{A_0(-Z_e\omega + iZ_a c\gamma)}{e^{-\gamma L}(-Z_e\omega + iZ_a c\gamma) - e^{\gamma L}(Z_e\omega + iZ_a c\gamma)}. \quad (7)$$

In this way the acoustic waves in the calibration tube are described by Eqs. (2), (3), (6), (7), within the limits of this steady state, linear oscillation model with simplified damping. However, there are unknown parameters to be imposed, or to be determined by measurements, in order to determine the waves at the microphone positions. These parameters are  $c$ ,  $Z_a$ ,  $\zeta$ ,  $Z_e$ ,  $L$  and  $A_0$ .

The amplitude of the pressure excitation  $A_0$  and the length of the tube  $L$  can be eliminated by considering pressure ratios along the tube. This defines the transfer function (TF)  $H_{m,n}$  between two microphones at position  $x_m$  and  $x_n$ :

$$H_{m,n} = \frac{p'(x_n, t)}{p'(x_m, t)}. \quad (8)$$

For the calibration setup in Fig. 1 we compute the TF using the indices  $n$  and  $m$  from either sets  $\{1..16\}$  or  $\{17..32\}$ . (i.e. Two microphones from different sides of the tube are not used to evaluate transfer functions.) Substituting  $A$  and  $B$  into Eq. (2) and simplifying, the transfer function between microphones  $m$  and  $n$  can be expressed independently of the excitation parameters, as follows:

$$H_{m,n} = \frac{f_n(Z_e\omega + iZ_a c\gamma) + f_n^{-1}(Z_e\omega - iZ_a c\gamma)}{f_m(Z_e\omega + iZ_a c\gamma) + f_m^{-1}(Z_e\omega - iZ_a c\gamma)}, \quad (9)$$

where an additional function  $f_a = e^{\gamma x_a}$  is defined for compact notations. The index  $a$  is used to select the appropriate microphone position in the expression.

## 3. Calibration methods

Depending on the way the wave guide model is adapted for calibration, various calibration methodologies can be obtained. Every methodology is based on the determination or elimination of the unknown parameters by using reference measurements. Because of the different initial assumptions and measurement uncertainties, the calibration accuracy can vary from method to method. In order to examine this effect, and present the way of choosing the most appropriate method, three different methods will be discussed and compared in the following.

Because of the uniform  $\Delta x$  spacing of the microphones any microphone position  $x_l$  can be expressed relative to the first microphone (denoted as  $mic_1$  in Fig. 1), located at position  $x_1$ :

$$x_l = \begin{cases} x_1 + (l - 1)\Delta x & \text{if } l \in \{1..16\} \\ x_1 + (l - 17)\Delta x & \text{if } l \in \{17..32\} \end{cases} \quad (10)$$

for the first or second side of the waveguide, respectively. This will be utilized in later equations.

### 3.1. Transfer function propagation method

A calibration method can be obtained if all the unknown parameters are eliminated by writing Eq. (9) for three subsequent microphone positions. The derivation of the formulation for this method can be found in Appendix. The transfer function between two microphones in a row can be directly computed from two transfer functions at the preceding positions. (e.g.  $H_{15,16}$  can be computed from  $H_{14,15}$  and  $H_{13,14}$ ) In this way, the transfer functions can be propagated along the tube and transfer functions of any microphone can be expressed relative to a reference microphone (e.g.  $mic_1$ ).

### 3.2. Parameterized transfer function model

Another method can be formulated as follows. The closure impedance,  $Z_e$ , (at position,  $x = 0$ ) can be ex-

pressed by the usual two microphone method by using Eq. (9). Using the transfer function  $H_{l,l+1}$ , formed by the signals of two subsequent, calibrated microphones at position,  $x_l$  and  $x_{l+1}$ ,  $Z_e$  can be written as:

$$Z_e = \frac{-iZ_a c \gamma (-H_{l,l+1} f_l + H_{l,l+1} f_l^{-1} + g f_l - (g f_l)^{-1})}{\omega (-H_{l,l+1} f_l - H_{l,l+1} f_l^{-1} + g f_l + (g f_l)^{-1})}, \quad (11)$$

where  $g = e^{\gamma \Delta x}$  is defined for the sake of compact notation.

Because  $H_{l,l+1}$ , as a function of  $\omega$ , is known from a measurement, the closure impedance depends on five additional, yet unknown parameters:  $x_1$ ,  $\Delta x$ ,  $\zeta$ ,  $c$ ,  $Z_a$ . In order to reduce the number of unknown parameters, Eq. (11) is inserted into Eq. (9), while substituting  $m = q$  and  $n = q + 1$ , yielding to the transfer function:

$$H_{q,q+1} = \frac{H_{l,l+1}(h_{q,l}g - h_{l,q}g^{-1}) + h_{l,q} - h_{q,l}}{H_{l,l+1}(h_{q,l} - h_{l,q}) + h_{l,q}g - h_{q,l}g^{-1}}, \quad (12)$$

where the function  $h_{a,b}$  is introduced for each pair of  $a$ ,  $b$  as:

$$h_{a,b} = f_a f_b^{-1} = e^{\gamma(x_a - x_b)} \quad (13)$$

Equation (12) contains a reduced number of unknown parameters  $\Delta x$ ,  $c$ ,  $\zeta$  (the last two are embedded in  $\gamma$ ). Note that the parameter  $x_1$ , which is implicitly defined in Eq. (12) via Eq. (10), (13), is also unknown. However, Eq. (12) is invariant when  $x_q$  and  $x_l$  are shifted by the same amount shown explicitly in Eq. (13). Consequently, the parameter  $x_1$  can be chosen arbitrary in this model. Therefore  $x_1 \equiv 0$  will be used for the parameter estimation. This equation represents the basis of the calibration methodology, because it connects two transfer functions via the unknown parameters that are constant for all transfer functions along the waveguide.

These three unknown model parameter can be estimated by considering that the proper parameter combination should give the smallest difference between a measured  $H_{q,q+1}$  and a predicted  $H_{q,q+1}^p$  transfer function. The latter is obtained by substituting measured  $H_{l,l+1}$  and the estimations of the model parameters into the right-hand side of Eq. (12).

This type of parameter estimation problem can be formulated as follows:

$$\Theta = \operatorname{argmin} \left( \sum_{o=1}^{N_{sp}} \|H_{q,q+1}^p(\omega_o) - H_{q,q+1}(\omega_o)\|_2 \right), \quad (14)$$

where  $N_{sp}$  is the number of samples in the measured discrete transfer function  $H_{q,q+1}$ ,  $\|\cdot\|_2$  denotes the Euclidean norm. The parameter values, for which the sum of the norm of the differences is minimal, is returned by  $\operatorname{argmin}$  and therefore,  $\Theta$  is a vector (the minimizer) that contains the estimated parameters. The solution can be obtained with a non-linear least-squares method, or similar optimization method. In this study

the Levenberg-Marquardt (L-M) iterative algorithm is used to solve the problem. The algorithm needs the derivatives of Eq. (12) with respect to the unknown parameters, which can be analytically computed in this case. The iteration is started with an initial guess. Due to the fact that the algorithm computes only the local minimizer of Eq. (14) the initial guess of the parameters has to be close to the solution. It is reasonably easy to find a good initial guess, because the parameters are measurable physical quantities. With the exception of the damping coefficient,  $\zeta$ , the parameters can be approximated with relatively simple measurements. The estimation is performed simultaneously for both the real and imaginary part of the transfer function.

The estimation procedure of the unknown parameters requires two accurate transfer functions. Therefore, at least three subsequent, calibrated microphone signals are necessary. To improve the accuracy of the results, it is possible to perform the fit simultaneously for more than two measured transfer functions. However, this significantly increases the cost of the fitting procedure. In this work, the estimation algorithm was stopped when the residual sum of subsequent parameter changes was below  $10^{-5}$ , or the number of iterations exceeded 60.

### 3.3. Alternative transfer function parameterization

By following the derivation in Sec. 3, an alternative methodology for the transfer function parameterization can be proposed. If the end impedance  $Z_e$  is not inserted into Eq. (9) in analytical form, but instead it is computed from a measured transfer function,  $H_{l,l+1}$ , the parameters  $Z_a$  and  $x_1$  are not eliminated for the fit of Eq. (12). Therefore, five unknown parameters should be estimated by the Levenberg-Marquardt algorithm. In this case, the update of the predicted transfer function,  $H_{q,q+1}^p$ , is performed in two steps. First, the current parameter estimates are used to compute  $Z_e$ , then the model TF is computed and the residuals are updated. This method rises the possibility to use averaged  $Z_e$ , computed from several measured transfer functions  $H_{l,l+1}$ , for the parameter estimation.

## 4. The measurement chain and reference calibration

The calibration setup is depicted in Fig. 1, with 32 microphones. The calibrations were performed with Knowles PG-23329 miniature electret microphones, used by the authors for beamforming purposes. In all subsequent results, bandpass filters, with a frequency band of [20 Hz–20 kHz], have been used. The performance of the algorithms is measured by comparing the deviations of the calibration factors from the calibration factors obtained by a reference calibration. This section overview the processing and reference calibra-

tion methods and presents the general characteristics of the microphones for which the calibration will be performed.

4.1. The parameters of the acquisition

The impedance tube was excited with a logarithmically swept sinusoid, having variable amplitude in order to keep the acoustic amplitude approximately constant in the swept frequency band. Without this compensation the signal amplitude in the tube would strongly vary with frequency due to the effect of pipe resonances. The signal bandwidth was from 100 Hz to 4.8 kHz, and the length of the sweep was 1.5 s. In order to estimate the transfer functions, discrete time samplings,  $\tilde{\mathbf{y}}^v$ , of the microphone signals are considered at positions,  $x_m$  and  $x_n$ . The elements, of each realization of  $\tilde{\mathbf{y}}^v$  ( $v = 1..V$  where,  $V$  is the number of time series acquired), corresponds to regularly sampled signal, with the sampling frequency,  $f_s$ . The discrete Fourier transformation is used to convert each block data  $v$  to the spectral domain. The element  $o$  of the Fourier transformed signal  $\mathbf{y}^v$  is computed as:

$$y_o^v = \frac{1}{N_{sp}W} \sum_{n=1}^{N_{sp}} \mathbf{w}_n \tilde{\mathbf{y}}_n^v e^{-i2\pi \frac{n-1}{N_{sp}}(o-1)}, \quad (15)$$

where  $o = 1..N_{sp}$  and  $N_{sp}$  is the number of samples in the time series  $v$ . The vector of window coefficients is  $\mathbf{w}$ , and  $W$  is the amplitude correction factor for the window. The cross spectrum of microphones at  $x_m$  and  $x_n$  then created by averaging procedure:

$$\mathbf{C}_{mn} = \frac{1}{V} \sum_{v=1}^V \mathbf{y}_m^v \mathbf{y}_n^{v\dagger}. \quad (16)$$

The transfer function between the two signals can then be expressed by

$$\mathbf{H}_{nm} = \frac{\mathbf{C}_{mn}}{\mathbf{C}_{mm}}. \quad (17)$$

The averaging of  $V$  segments of data helps decrease the contribution of the uncorrelated random noise.

During the measurements the sampling frequency was set to  $f_s = 65536$  Hz. The processing was done with  $N_{sp} = 32768$  samples. The data segments  $\tilde{\mathbf{y}}^v$  of the measurement are defined with an overlap of 50% of  $N_{sp}$ . The Hanning window is applied to each data segment. The number of averages,  $V$ , were 120 in case of the reference calibration of the microphones and it was 69 in every other measurement cases.

4.2. The reference calibration methodology

The reference calibration technique is also implemented on the impedance tube setup shown in Fig. 1. The  $Z_e$  termination is removed and four electret microphones and a reference Brüel & Kjør (B&K) 4191

microphone are flush mounted at the end of the tube using a rigid end plate. The microphones are supposed to sense exactly the same acoustic field, up to the cut-on frequency of the first non-planar mode of the tube at  $f_c \cong 4.6$  kHz. The magnitude and phase characteristics of four microphones can be seen in Fig. 2, as compared to the B&K microphone.

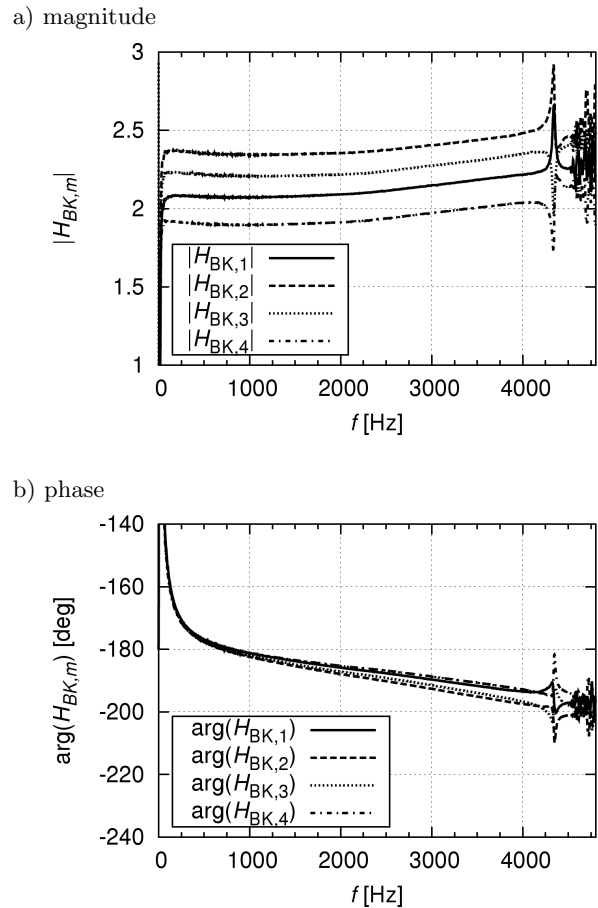


Fig. 2. Response of the electret microphones, in comparison with the B&K reference microphone.

Significant discrepancies between the microphone sensitivities can be observed. The phase plots show the different time delay of the microphone channels, as indicated by the phase mismatches. Using these transfer functions, the microphone correction factors are computed and microphone signals are calibrated with respect to one reference. In the present case this reference microphone is microphone  $mic_1$  (Fig. 1).

The modulus and phase of the transfer function between microphone 2 and 1 is plotted in Fig. 3. The uncertainties are also indicated. This data is computed from five measurements with varying signal to noise ratios and amplifier gain settings. The uncertainties are related to 95% confidence level. The uncertainty of the modulus of the transfer function is approximately 2% in the range of 100 Hz to 4.6 kHz, while the uncertainty of phase is approximately  $\pm 0.6^\circ$ .

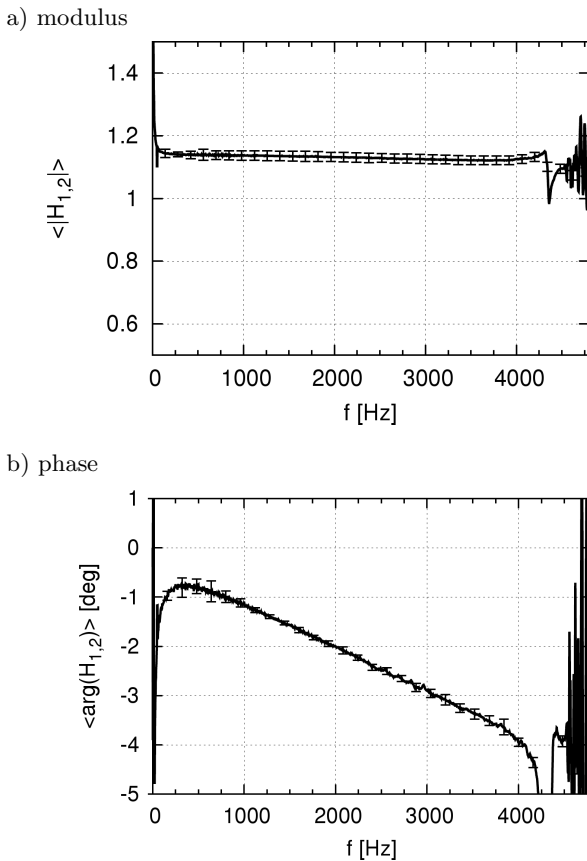


Fig. 3. Transfer functions and uncertainties with 95% confidence interval, obtained with the reference microphone calibration.  $\langle \cdot \rangle$  denotes ensemble average.

The reference calibration shows  $m$  and  $n$  that the impedance tube can be used to perform accurate measurements up to 4.6 kHz. Rapid change of microphone amplitude and phase characteristic is shown around 4.4 kHz. This behaviour is also observed in free field calibration of the microphones, therefore, it is related to the microphones and not to the reference calibration method. Because of the possible sensitivity of this part of the curve to changes in environmental conditions, we restrict our analysis to a maximum frequency of 4.2 kHz.

Note also, that the time delay between channel 1 and 2 can be approximately estimated from the linear part of the phase plot. This estimation gives  $3 \mu\text{s}$  delay between the two channel, which would lead to about  $20^\circ$  phase difference at 20 kHz, therefore phase calibration is recommended.

#### 4.3. The measured transfer functions

The transfer functions measured between microphone positions 1 and 2 and between 17 and 18 are depicted in Fig. 4, in the form of the real and the imaginary part. These transfer functions are obtained at the same axial position of the tube but the pairs of microphones are located on opposite sides of the tube.

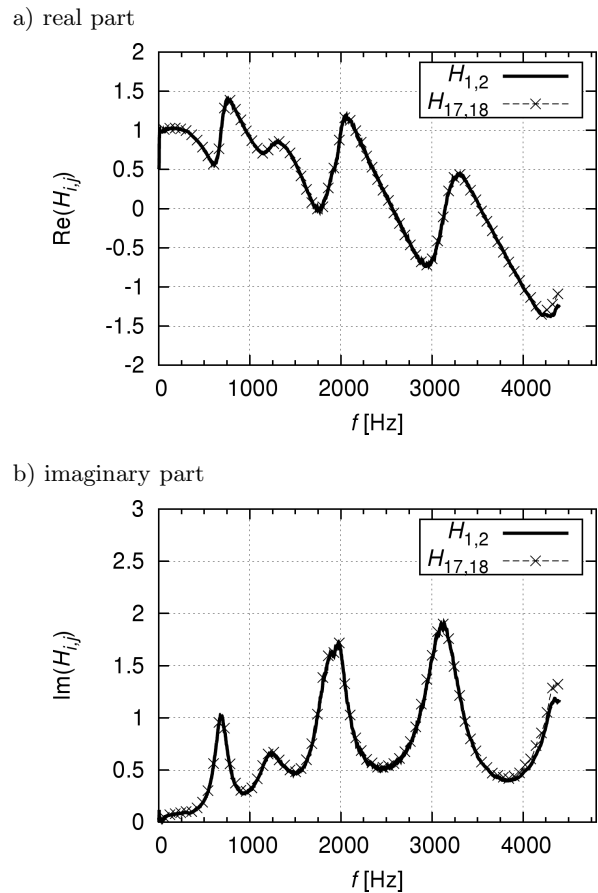


Fig. 4. The transfer function measured with calibrated microphones. Microphone pairs 1, 2 and 17, 18 are located at the same axial position but at opposite sides of the tube.

Very good agreement between the real and imaginary parts indicates the accurate microphone positioning on both sides of the tube, as well as the plane wave propagation in the tube. It also indicates that the microphones reference calibration is not altered during the assembly into the tube. The plot confirms the previously mentioned problem of the microphone response around 4.4 kHz, where microphone characteristics are not smooth and the difference between the curves becomes visible starting from 4–4.2 kHz.

## 5. Comparison of the parameterization methods

In order to indicate the differences between the prediction and the measured values, the amplitude and phase difference is introduced between the transfer function  $H_{1,q}$ , measured by calibrated microphones and the predicted transfer function  $H_{1,q}^p$ . As indicated by the indexes these transfer functions are always computed by using  $mic_1$  (Fig. 1), which is chosen as the reference microphone for the relative calibrations:

$$C_q^{\text{err}} = \frac{|H_{1,q}^p|}{|H_{1,q}|}, \quad (18)$$

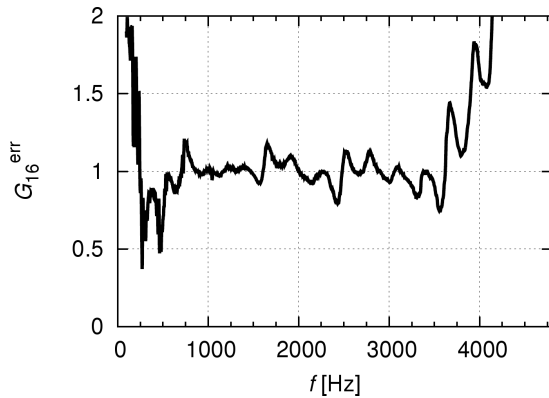
$$\phi_q^{\text{err}} = \arg(H_{1,q}^p) - \arg(H_{1,q}), \quad (19)$$

which give the amplitude and phase errors, as compared to the reference calibrated values. In the following section the calibration accuracy is evaluated at microphone position  $q = 16$ .

### 5.1. Transfer function propagation

The transfer function propagation method (Subsec. 3.1) does not need estimation of parameters, therefore it is the easiest method to use. Using the measured transfer functions,  $H_{1,2}$  and  $H_{2,3}$ , and Eq. (24), (25) the predicted error is shown in Fig. 5, for the microphone at position  $q = 16$ . The prediction error is large, possibly because the formulation propagates and amplifies the initial measurement error in  $H_{1,2}$  and  $H_{2,3}$ .

a) amplitude error



b) phase error

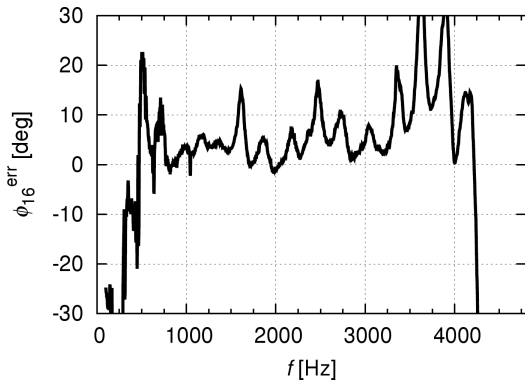


Fig. 5. The prediction error at microphone position  $q = 16$  for the transfer function propagation method.

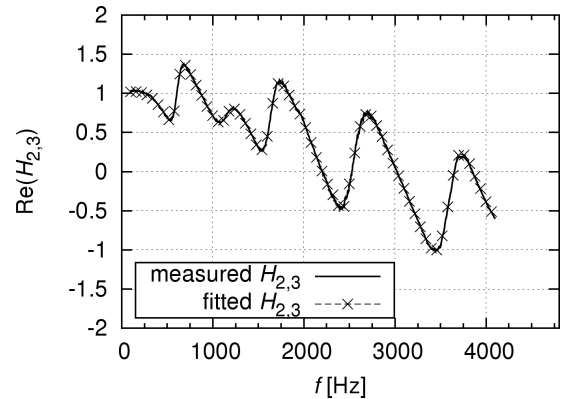
### 5.2. Parameterization with three parameters

Following the methodology presented in Subsec. 3.2, three unknown parameters are determined from the measurements. The estimation is based on two measured transfer function pairs  $H_{1,2}$ ,  $H_{2,3}$  and  $H_{17,18}$ ,  $H_{18,19}$ . Therefore, the estimation is performed for transfer functions on both sides of the tube, by averaging together the measured transfer functions at the

same axial positions. It is shown in Fig. 4 that significant mismatches between transfer functions on the opposite side of the tube can not be observed. Therefore, a large part of the frequency range is not affected by this averaging. The parameter estimation is performed by using the real and imaginary part of Eq. (12) simultaneously. The iterations of the L-M algorithm is started with several different initial parameters, and the resulting parameters those giving the smallest residues is chosen as the final parameter combination. This means that a direct search method, combined with the L-M algorithm is used. Every possible combination of 8 discrete equally spaced parameter values is used as an initial parameter for the L-M method from the intervals of  $330 \leq c \leq 355$ ,  $0.028 \leq \Delta x \leq 0.032$ ,  $1 \times 10^{-6} \leq \zeta \leq 1 \times 10^{-1}$ . The resulting fitted parameters are  $c = 342.7$  m/s,  $\Delta x = 0.03021$  m,  $\zeta = 0.01302$ .

The estimated transfer function curve can be observed in Fig. 6. The agreement with the transfer function measured by calibrated microphones is excellent.

a) real part



b) imaginary part

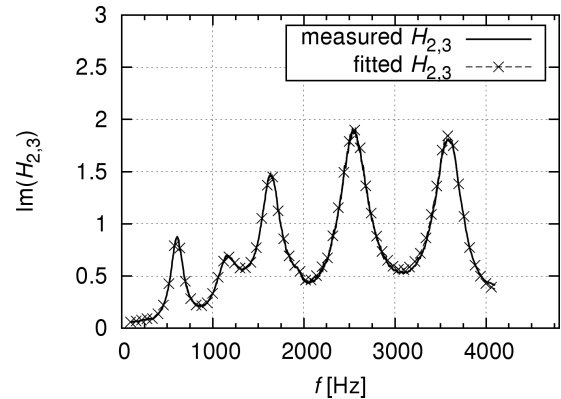


Fig. 6. The measured and fitted transfer function  $H_{2,3}$ .

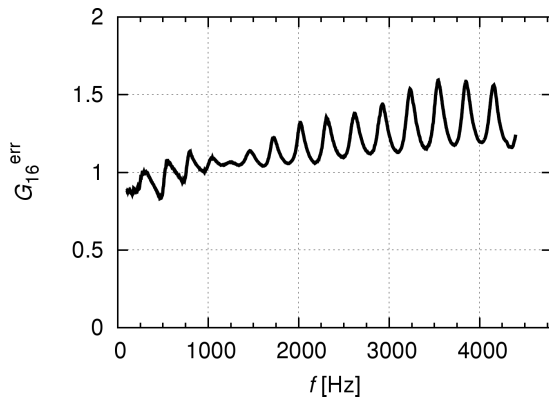
To compute the predicted transfer function, Eq. (11) and Eq. (10) are substituted into Eq. (9), and the reference microphone,  $mic_1$ , position is fixed:

$$H_{1,q}^p = \frac{H_{l,l+1}^m (g^{q-l} - g^{l-q}) + g^{l-q+1} - g^{q-l-1}}{H_{l,l+1}^m (g^{1-l} - g^{l-1}) - g^l + g^{-l}}. \quad (20)$$

In the current set-up, the measured transfer function,  $H_{l,l+1}^m$ , is the average of  $H_{1,2}$  and  $H_{17,18}$ , specified at the same axial positions, but on opposite sides of the tube. The averaging was used to try to further decrease the effect of the small amount of differences between the transfer functions and the superimposed noise. However, it was found that this does not significantly increase the accuracy of the prediction and does not reduce the effect of noise, because of the mentioned very good agreement between  $H_{1,2}$  and  $H_{17,18}$ .

The prediction error for the transfer function can be seen in Fig. 7. The error is significant both in amplitude and phase value.

a) amplitude error



b) phase error

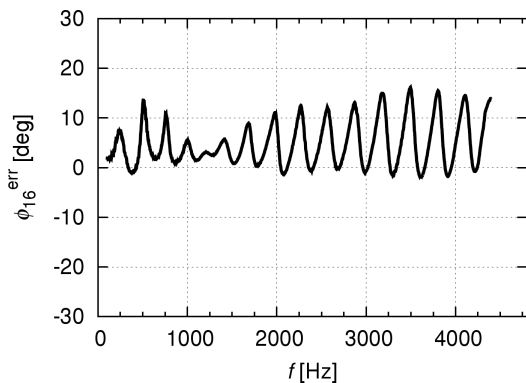


Fig. 7. The prediction error at microphone position  $q = 16$ .

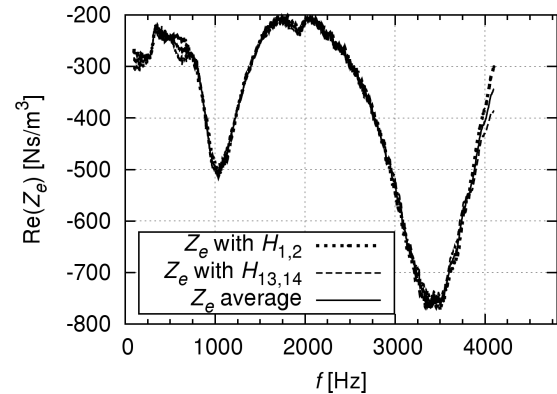
### 5.3. Alternative parameterization with five parameters

The calibration accuracy obtained with the alternative parameterization (Subsec. 3.3) is verified here.

In order to increase the accuracy,  $Z_e$  is used as an averaged value computed from several different transfer functions along the tube. In the present case, two transfer functions,  $H_{1,2}$  and  $H_{13,14}$ , are used for calculating  $Z_e$ . Due to the increased number of parameters (five instead of three), the convergence of the iterative method is more sensitive to the correct choice of initial parameters. Similarly to the previous fitting methodology, the iterative algorithm is combined with

a direct search method, by launching the L-M algorithm with several different initial conditions. It was found that indeed there are more unconverged runs, meaning that solutions are not obtained for the prescribed tolerance within the 60 iterative steps. This typically happens when the initial point is far from the parameter combination result with the smallest residuals. It was also observed, that performing the minimization separately on the real or on the imaginary part of the transfer function is slightly more robust than performing it simultaneously on both. This behaviour was not observed for the previous estimation methodology with three free parameters. The parameter estimation is performed with residuals minimized for transfer function  $H_{3,4}$ . The obtained parameters are the following:  $c = 340.0$  m/s,  $x_1 = 0.1819$  m,  $\Delta x = 0.02971$  m,  $Z_a = 404.2$  kg/m<sup>2</sup>/s,  $\zeta = 0.00504$ . Using these parameters the real and imaginary parts of the end impedance are plotted in Fig. 8.

a) real part



b) imaginary part

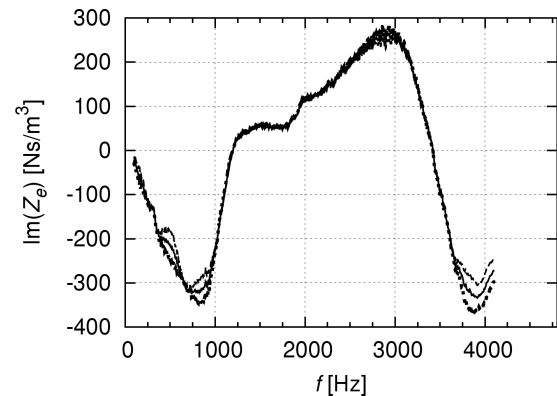


Fig. 8. Computed  $Z_e$  based on measured transfer functions  $H_{1,2}$  and  $H_{13,14}$ .

The measured and fitted transfer functions are compared in terms of real and imaginary parts in Fig. 9.

Finally, the resulting errors at microphone position  $q = 16$  are depicted in Fig. 10, showing that the errors are much less than with the three parameter estimation algorithm.

### 6. Discussion

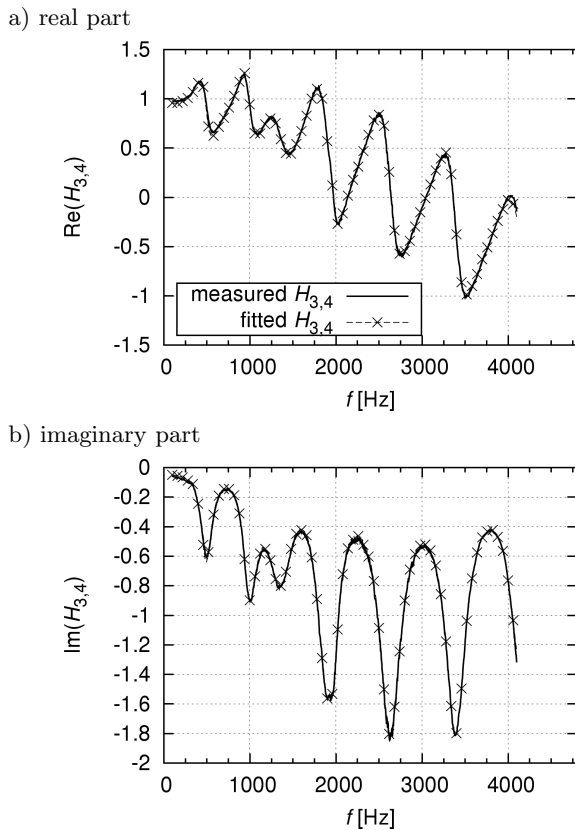


Fig. 9. Predicted  $H_{3,4}$ , based on fitted parameters, compared to the measured transfer function.

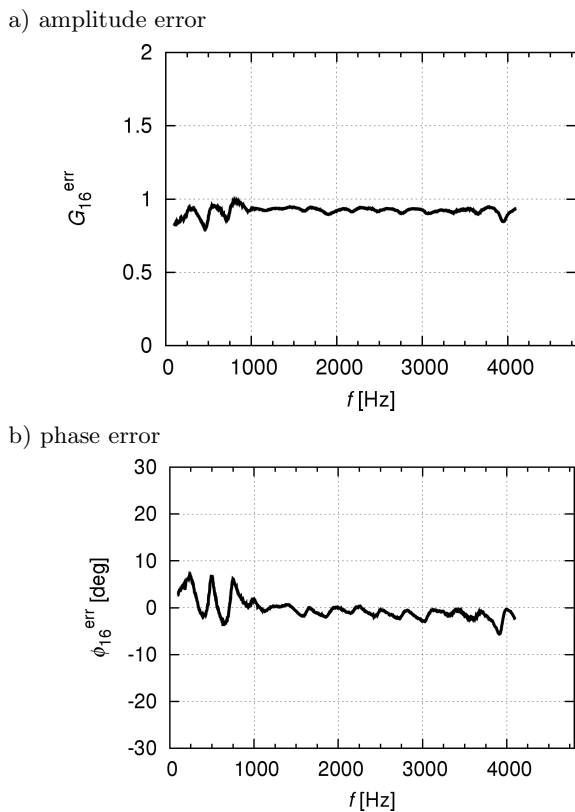


Fig. 10. The prediction error at microphone position  $q = 16$ , with the prediction method using a computed value for  $Z_e$  (shown in Fig. 8).

The presented algorithms show different calibration accuracy. The transfer function propagation method is the easiest to use, because no parameter estimation is needed. However, it accumulates errors, and at farther positions from the reference microphone these accumulated errors can be huge and can ruin the calibration.

Prediction accuracy can be improved by using the parameter estimation method. The calibration methodology based on three parameters is the easiest to converge and gives better calibration accuracy. It can be observed that the amplitudes of the error are fluctuating with frequency. The amplitude error is increases with frequency and for the phase error, an average bias of approximately 2–5 deg can be observed. This average constant error is better than a constantly increasing phase shift for array processing. However, this level of accuracy is still not acceptable for many applications, especially for narrowband processing, where the rapid fluctuation of phase error is a problem.

The calibration method, using five fit parameters and averaged  $Z_e$ , computed from two measured transfer functions, gives a much smaller error. Instead of linearly increasing error the amplitude has a bias error. The microphone sensitivity, at all frequencies, is under predicted by 5–10%. In terms of the phase error, the average bias is almost disappeared. Below 1 kHz, significant oscillatory behaviour can still be observed with a phase mismatch approaching  $\pm 8$  deg. Above 1 kHz, the phase error is smaller than  $\pm 3$  deg with the exception of a small peak at 3.9 kHz.

In both parameter estimation methods, especially in the transfer function propagation method, the calibration error depends on the relative position of the microphones used for the parameter fitting and the microphone to be calibrated. Measurements showed that the farther they are from each other the higher is the phase and amplitude error. In the presented cases, the microphone to be calibrated is at the farthest possible position ( $q = 16$ ) from the fitted transfer function. Therefore, the tests investigate the worst possible scenario in terms of accuracy, which can happen on this particular set-up. In the five parameter estimation method the situation is improved, as compared to the three parameter fit model, because for the  $Z_e$  calculation, one of the transfer functions is chosen to be close to the end of the row. This improved the results, but it has to be noted that the errors of this method are still significantly smaller when the transfer functions for the  $Z_e$  computation are chosen from the first microphone positions of the tube. The five parameter fit method gives smaller phase and magnitude errors, which, for example, can be acceptable for beamforming applications.

The calibration errors also point out that the model of the wave propagation is not perfectly predict the

real propagation. The model include neither the unintended effects of the microphone mounts along the tube nor the non-perfect closure of the tube. The closure impedance at the end of the calibration tube was not perfectly aligned, because damping foam was inserted between the calibration tube and the closure segment. Therefore, this could cause a slight misalignment of the attached perforated damping tube section. Some uncertainty of the measurement may be introduced as a result of this. Precise closure of the tube and simpler microphone mounts would have possibly improve the calibration accuracy of the presented methods.

## 7. Conclusion

The paper presents an investigation on the accuracy of the simultaneous calibration of several (32) electret microphones in an impedance tube. The calibration can be performed with different strategies, of which three are described and compared, regarding accuracy and processing complexity. The calibration arrangement allows the calibration of tens of microphones in one measurement.

All the methods are based on the analytical model of damped plane wave propagation in a duct. The models contain several unknown parameters, depending on the assumptions and simplifications made for the measurement procedure. All procedures require a minimum of 3 pre-calibrated microphones in order to obtain two transfer functions along the tube. The pre-calibration of a few microphones is done in the same facility, with a small uncertainty, as it has been shown in the paper.

One of the calibration procedures is a subsequent transfer function computation method without model parameters. This method strongly amplifies the measurement errors of the initial transfer functions. This method is not recommended for practical use.

The other two procedures use the Levenberg-Marquardt algorithm to estimate the propagation parameters of the model.

Their comparison showed that the one with five free parameters gives the smallest calibration errors. However, the convergence of the algorithm was slightly more difficult than in the case of the three free parameter model. The accuracy of the five parameter model is improved by computing the averaged  $Z_e$  from transfer functions measured at the beginning and at the end of the row of microphones. Therefore, this method requires at least four pre-calibrated microphones. The calibration phase error was everywhere in the range of approximately  $\pm 8$  deg, above 1 kHz it is approximately in the range of  $\pm 3$  deg. The amplitude mismatch was approximately 10% maximum, and approximately 5% above 1 kHz.

## Appendix.

### Transfer function propagation method

If the distance between the consecutive microphones is the same along the wave guide, all the unknown parameters can be eliminated and the transfer function between subsequent microphones can be expressed from two known subsequent transfer functions. This technique therefore requires 3 calibrated microphones and no parameter estimation technique. The method is as follows:

$$H_{l+1,l+2} = g - \frac{1}{H_{l,l+1}} + \frac{1}{g}. \quad (21)$$

The distance between the microphones  $\Delta x$  can be written as:

$$j = \sqrt{a^*}, \quad (22)$$

where

$$a^* = H_{l+1,l+2}^2 H_{l,l+1}^2 + 2H_{l+1,l+2} H_{l,l+1} + 1 - 4H_{l,l+1}^2, \quad (23)$$

$$\Delta x = \frac{1}{\gamma} \ln \left( \frac{H_{l+1,l+2} H_{l,l+1} + 1 \pm j}{2H_{l,l+1}} \right).$$

Substituting  $Z_e$  and  $\Delta x$  into the transfer function  $H_{l+2,l+3}$  (Eq. (9)) leads to the following expression:

$$H_{l+2,l+3} = \frac{H_{l+1,l+2}^2 H_{l,l+1} - H_{l,l+1} + H_{l+1,l+2}}{H_{l+1,l+2} H_{l,l+1}}. \quad (24)$$

This closed form solution can be used iteratively on all the subsequent microphones mounted along the wave guide, to determine the theoretical transfer function between them. The transfer function, relative to the first microphone, can be calculated as:

$$H_{1,q}^p = \prod_{l=1}^{q-1} H_{l,l+1}. \quad (25)$$

## Acknowledgments

The present work was supported by the European Commission, in the framework of the FP7 VALIANT project (Grant Agreement 233680). The authors are also grateful for the support of the Hungarian National Fund for Science and Research under contract No. OTKA K 83807 for the financial support provided during the writing of the paper.

## References

1. BLAUERT J., XIANG N. (2008), *Acoustics for Engineers*, Springer Berlin.
2. BOONEN R., SAS P., DESMET W., LAURIKS W., VERMEIR G. (2009), *Calibration of the two microphone transfer function method with hard wall impedance measurements at different reference sections*, Mechanical Systems and Signal Processing, **23**, 1662–1671.

3. DE ROECK W., NORDSTRM L., ENGLUND T., DESMET W. (2012), *Experimental two-port characterization of the aeroacoustic transmission properties of a truck's exhaust system*, Technical Report 2012-01-1558, SAE International.
4. HUMPHREYS W.M., GERHOLD C.H., ZUCKERWAR A.J., HERRING G.C., BARTRAM S.M. (2003), *Performance analysis of a cost-effective electret condenser microphone directional array*, 9th AIAA/CEAS Aeroacoustics Conference.
5. KULKA Z. (2011), *Advances in digitization of microphones and loudspeakers*, Archives of Acoustics, **36**, 419–436.
6. LOWIS C., JOSEPH P., SIJTSMA P. (2010), *A technique for the in situ phase calibration of in-duct axial microphone arrays*, Journal of Sound and Vibration, **329**, 4634–4642.
7. MUELLER T.J. Ed. (2002), *Aeroacoustic Measurements*, 1 edition, Springer, Berlin.
8. OLDHAM J.R., SAGERS J.D., BLOTTER J.D., SOMMERFELDT S.D., LEISHMAN T.W., GEE K.L. (2009), *Development of a multi-microphone calibrator*, Applied Acoustics, **70**, 790–798.
9. PAULRAJ A., KAILATH T. (1985), *Direction of arrival estimation by eigenstructure methods with unknown sensor gain and phase*, ICASSP'85, IEEE International Conference on Acoustics, Speech, and Signal Processing, 640–643, Tampa, FL, USA.
10. RAYKAR V., DURAIWAMI R. (2004), *Automatic position calibration of multiple microphones*, ICASSP'04, IEEE International Conference on Acoustics, Speech, and Signal Processing, **4**, 69–72.
11. SNG Y.H., LI Y. (2000), *Fast algorithm for gain and phase error calibration of linear equi-spaced (LES) array*, WCC 2000 – ICSP 2000, 5th International Conference on Signal Processing, 16th World Computer Congress, pp. 441–444, Beijing, China.
12. TASHEV I. (2005), *Beamformer sensitivity to microphone manufacturing tolerances*, Proceedings of Nineteenth International Conference Systems for Automation of Engineering and Research SAER 2005, St. Konstantin Resort, Bulgaria.
13. WYLIE E.B., STREETER V.L. (1978), *Fluid Transients*, McGraw-Hill Inc.
14. YARDIBI T., BAHR C., ZAWODNY N., LIU F., CATTAFESTA III L.N., LI J. (2010), *Uncertainty analysis of the standard delay-and-sum beamformer and array calibration*, Journal of Sound and Vibration, **329**, 2654–2682.
15. ZUCKERWAR A.J., HERRING G.C., ELBING B.R. (2006), *Calibration of the pressure sensitivity of microphones by a free-field method at frequencies up to 80 khz*, The Journal of the Acoustical Society of America, **119**, 320–329.